PHYSICAL REVIEW E VOLUME 61, NUMBER 5 MAY 2000

Effect of wall deformations on a confined fluid

J. Chakrabarti*
Laboratory of Separation Processes and Transport Phenomena, P.O. Box 513, 5600 MB Eindhoven, The Netherlands
(Received 6 May 1999; revised manuscript received 4 February 2000)

We investigate the effect of wall deformations on a fluid confined in a slit of deformable walls. Monte Carlo (MC) simulations show that the fluid undergoes rarefaction or condensation depending on the wall rigidity for a small wall separation. The slope of the mean squared displacement as a function of MC steps has an algebraic dependence on the wall rigidity. The simulated density profile is qualitatively accounted for by means of a mean-field theory.

PACS number(s): 61.20.Ja

Intriguingly rich phase behaviors of a fluid in confined geometries [1] are challenging in statistical mechanics due to tremendous density inhomogenity induced by the confining walls. Extensive laboratory experiments and theoretical studies, using density functional theories and computer simulations on model Lennard-Jones (LJ) systems [where the particles interact via a spherically symmetric potential, given by $v_{LJ}(r)=4\epsilon[(\sigma/r)^{12}-(\sigma/r)^{6}]$, ϵ being the depth of the interaction and σ being the range over which the potential is repulsive] confined by idealized hard or soft [i.e., the wall-particle intercation having a long repulsive or attractive tail, respectively] walls have yielded useful insight into such systems [2]. Nevertheless, the walls encountered in reality may deviate considerably from these idealized walls. For instance, the effects of wall roughness have been investigated recently [3]. None of these studies, however, focus on the effect of the wall (shape, etc.) deformability on the phase behavior of the intervening fluid. There have been recent experimental studies [4] on a system where a colloidal suspension of micrometer-size polystyrene latex particles has been confined in foam films. Such systems can be thought of as prototypes of fluids confined by a pair of deformable walls. There are ample examples of such systems, namely, a fluid confined between two interfaces. The effect of the wall deformations could be important in the context of biological systems as well, where the transport of the fluids takes place through narrow channels of deformable walls.

Model

Here we study a simple model incorporating the effect of the wall deformations. Let us consider a system of LJ particles in a slit geometry with walls at $z=\pm H/2$, where z is normal to the plane of the walls. The wall is treated as an elastic continuum. A LJ particle, viewed as a sphere of diameter σ $(=2a)$, will stretch the wall as it approaches the wall within a separation equal to or less than its radius. We consider only the normal component of the strain generated in the wall [5], which reduces it to a simple one-dimensional problem. The wall-particle interaction in this model is treated simply in terms of energy difference between various configurations, specifically, the one where the particles fill positions normally occupied by the wall and the one where they are well away from the wall. This is inspired by a typical situation shown in Fig. 1(a). The original wall position is the chord $(=2l)$ of a circle, shown by the dashed line, and the deformed wall will take the shape of an arc $(=2s)$. If d is the distance of the center of the particle from the original wall, $l=(a^2-d^2)^{1/2}$. Moreover, if the angle, θ tended by s at the center is small, $s=a\cos^{-1}(a/d)$. Since a particle can penetrate the wall, the center can lie within the bounds of $\pm|H|/2$ and outside, as well. In the former case $d=|H/2|-|z|$, and the wall deformation δ_1, the difference in length between the arc and the chord, is $2(s-l)$. In the latter case $d=|z|-|H/2|$ and the deformation $\delta_2=2\pi-2(s-l)$. Let us assume that the stress generated by the wall to relax the deformation would follow Hooke's law. The energy cost of this stress would act like an external potential on the confined fluid and would be given for a particle at z by $V_{ext}(z)=K\delta_1^2$ for $(H/2-|z|)\leqslant\frac{1}{2}$; $=K\delta_2^2$ for $(|z|-H/2)<\frac{1}{2}$; $V_{ext}(|z|=H/2+\frac{1}{2})=\infty$; and $V_{ext}(z)=0$ otherwise. Here K is the stretching modulus of the wall. The unit of length is σ, the temperature scaled according to k_BT/ϵ and, accordingly, $K^*=K\sigma^2/\epsilon$ [6]. Typical plots of $V_{ext}(z)$ have been shown in Fig. 1(b) for both a high and a low K^* [7]. The roughness of the wall, resulting from cooperative colli-

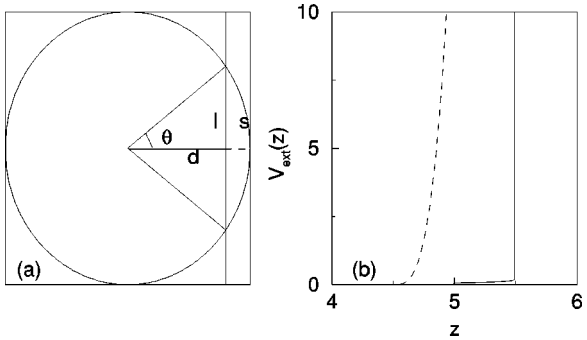

FIG. 1. (a) Model of the wall deformation [one symmetric half]: l denotes the original wall, s the deformed wall, d the distance of the center of the particle from the original wall, and θ the angle of s at the center. The dashed continuation of d is to make s more prominent to the eyes. (b) Sketches of the external potential $V_{ext}(z)$ as a function of z for wall rigidity modulus, $K^*=0.01$ (solid line) and $K^*=100$ (dashed line).

*Permanent address: S. N. Bose National Centre for Basic Sciences, Block-JD, Sector III, Salt Lake, Calcutta 700 091, India.

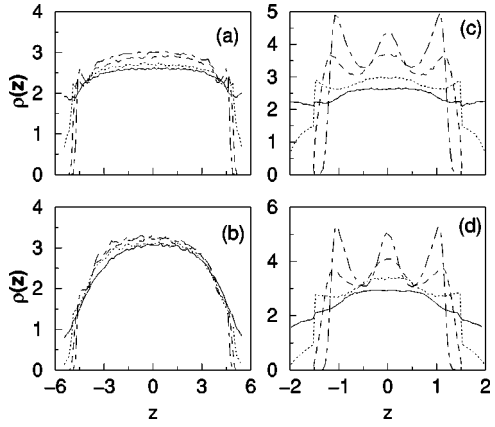

FIG. 2. Density profile $\rho(z)$ as a function of z (solid curve for $K^*=0.01$, dotted curve for $K^*=1.0$, dashed curve for $K^*=10$ and long-and-short dashed curve for $K^*=100$) for (a) $\rho_0\sigma^3=0.4$, $k_BT/\epsilon=2.0$ and (b) $\rho_0\sigma^3=0.5$, $k_BT/\epsilon=1.25$, both with $H=10$; (c) and (d) same conditions as for $\rho_0\sigma^3$, k_BT/ϵ as in (a) and (b), respectively, but with $H=3$.

sions by the particles, would be ignored. This roughness would occur at a length scale of the particle diameter. However, for a low density, where the mean particle separation exceeds the particle diameter and at a high temperature where the chance of particles being stuck at the wall is smaller, this roughness could be ignored, provided $H>\sigma$.

Monte Carlo simulations

The Monte Carlo (MC) simulations are performed by standard Metropolis algorithm on $N=192$ LJ particles at a bulk density $\rho_0\sigma^3$ and temperature k_BT/ϵ, subject to $V_{ext}(z)$ in a parallelepiped geometry having periodic boundary conditions (PBC) in the x-y directions with the ratio of the dimensions $L_x/L_y=\sqrt{3}/2$ and no PBC in the z direction. Note that unlike the earlier works [2,3], the wall has a dynamics due to the impinging particles. The dynamics of the wall (in the Monte Carlo sense) is implicitly accounted for here, that is, the wall (z) configuration has a Boltzmann weight according to the deformation energy cost given in terms of $V_{ext}(z)$; hence, the coupled system of the particles and the boundary evolve self-consistently to a steady state. The first 10 000 MC steps (each step being N attempts to move the particles) are discarded for reaching the steady state, which is checked by monitoring the energy E of the system. The next 10 000 steps are performed for calculating different quantities of interest, which are finally averaged over five independent runs.

We report the results from our simulations for two bulk parameters [8]: a bulk liquid phase below the critical point $\rho_0\sigma^3=0.5$, $k_BT/\epsilon=1.25$ and a bulk fluid phase above the critical point $\rho_0\sigma^3=0.4$, $k_BT/\epsilon=2.0$. Figures 2(a) and 2(b) show the density profiles $\rho(z)$ calculated by binning the z coordinates of the particles, for different K^* with $H=10$. Clearly in this case, irrespective of the bulk conditions, the density profiles show a very flat structureless peak at the center. For $H=3$, on the other hand, $\rho(z)$, shown in Figs. 2(c) and 2(d), exhibits pronounced peaked structures as K^* increases, indicating the formation of three layers for both the bulk conditions. The structure for large K^* can be understood from simple packing considerations as in the case

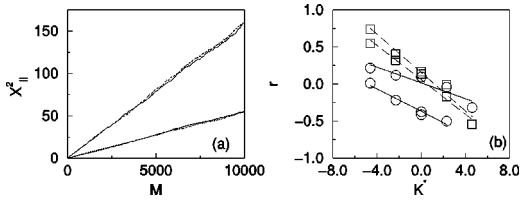

FIG. 3. (a) MSD in the x-y plane in the pore for the bulk liquid case with $H=3$ for $K^*=0.01$ (dashed line) and $K^*=100$ (dotted line). The solid lines correspond to the analogous quantity obtained from the bulk simulations with the same temperature but with ρ_{eff}. (b) Log-log plot of $r=S/S_0$ as a function of K^* for two different bulk conditions with $H=10$ (circles) and $H=3$ (boxes). The solid and the dashed lines show the best fit lines.

of a pair of fixed rough walls in Ref. [3]. This is quite expected, for in the large K^* regime the wall is less mobile due to the high energy cost of deformations. We note that the effective pore width H_{eff}, defined by the maximal z coordinate up to which $\rho(z)\neq 0$, is different from H and increases as K^* decreases.

The mean squared displacement (MSD) in the (x-y) plane parallel to the walls, $X_{||}^2$ $[=1/N\langle\Sigma_i[(x_i-x_i(0))^2+(y_i-y_i(0))^2]\rangle$, where (x_i,y_i) are the planar coordinates of the ith particle at a given MC step, $(x_i(0),y_i(0))$ is the initial positions, and the angular brackets denote averaging over the initial configurations] as a function of the MC steps, M [Fig. 3(a)] clearly confirms the liquid behavior within the pore [9]. We show in the same figure $X_{||}^2$ obtained by carrying out bulk simulations [with PBC in all three directions and without $V_{ext}(z)$] for the same temperature but at a rescaled density $\rho_{eff}=\rho_0 H/H_{eff}$. The matching of the MSD obtained in this way with those for the liquids in the pores clearly indicates that the liquid in the pore behaves as one with a bulk density equal to ρ_{eff}. Note that $\rho_{eff}<\rho_0$ if $H<H_{eff}$, indicating rarefaction of the liquid in the pore compared to the bulk situation. Clearly, for $H=3$, independent of the bulk conditions, the liquid in the pore exhibits rarefaction for a low K^* but undergoes condensation, i.e., $\rho_{eff}>\rho_0$ at a higher K^*. Comparing with the density profiles in Figs. 2(c) and 2(d), we note that while this change takes place, the density profile shows a transition from the broad central peak situation to a three-layered structure. The specific heat, defined by $1/N\langle(E-\langle E\rangle)^2\rangle$, as a function of K^* shows a peak at $K^*=0.1$, which grows with increasing lateral (x,y) dimensions ($N=432$), implying the existence of a thermodynamic transition. The large K^* behavior is reminiscent of the well-known capillary condensation [2]. Figure 3(b) shows another interesting feature of the system. We plot the ratio $r=S/S_0$, where S is the slope of the MSD as a function of MC steps for the liquid within the pore and S_0 that in the bulk condition, characterized by $(k_BT/\epsilon,\rho_0\sigma^3)$. Here r follows a power-law behavior: $r=r_0+A(K^*)^{-\alpha}$ with nonzero intercept r_0 as a function of K^*, where the exponent, α is found to depend on H (Table I), in agreement with our observation on the density profiles.

It is interesting to understand the density profile while the system undergoes rarefaction for $H=3$. Clearly, the loss of structure in the density profile cannot be understood by packing considerations. Even though $H_{eff}>H$ in such cases, the density profile cannot be explained solely by considering a

TABLE I. α for different cases.

Bulk condition	$H=10$	$H=3$
Liquid	0.05	0.12
Fluid	0.07	0.13

pore of larger width either. To illustrate this point, we carry out Monte Carlo simulations by switching off $V_{ext}(z)$, but confining the particles between two hard walls, namely, in an external potential $V_0\delta(z\pm H_{eff}/2)$, with $V_0=\infty$. The density profile, shown in Fig. 4(a), exhibits peaks close to the walls, quite unlike what we observe in the low K^* regime. We gain further insight as follows. Let us consider a high K^*, where the density profile shows a clear peak close to the wall. We pick up all the particles lying under this peak from different configurations and generate the histogram, $f(z_0)$ of $z_0=(1/N')\Sigma_i' z_i$, where the prime denotes that only the particles under the peak are being considered. Obviously, for a well-defined peak, this histogram will be sharp, as shown in Fig. 4(b). On the other hand, the histogram for the same quantity with the particles having $|z|\geq H/2$ for a low K^* deviates from the sharp feature, as in Fig. 4(c). This indicates that the density profile has a peak here, too, but its position fluctuates and gets washed out due to averaging over a large number of configurations. Since a pair of well-defined walls tends to build up peaked structures close to the walls for the conditions we consider here [Fig. 4(a)], the fluctuations in the peak position can be associated with those in the wall position itself for a low K^*. The wall fluctuations, triggered by the impinging particles, dominate this regime due to low

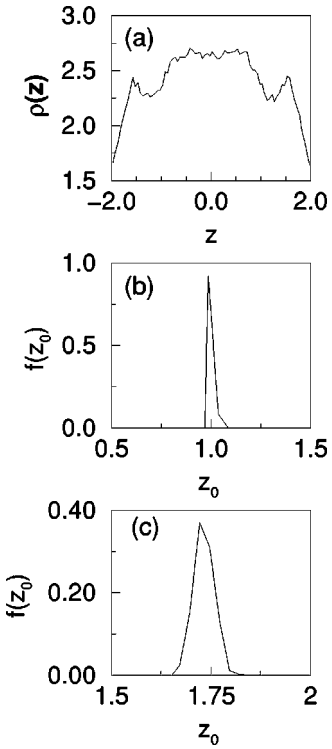

FIG. 4. For the bulk fluid condition with $H=3$: (a) $\rho(z)$ as a function of z for particles confined between a pair of hard walls at separation of H_{eff} corresponding to $K^*=0.01$; (b) the histogram, $f(z_0)$ of z_0 with $K^*=100$, and (c) that for $K^*=0.01$.

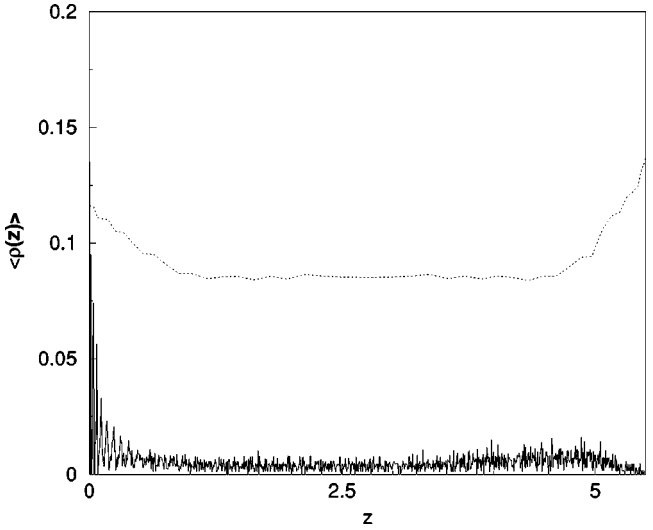

FIG. 5. Density profile, $\langle\rho(z)\rangle$ as a function of z, obtained by averaging over 100 realizations of the wall position in our mean-field theory. The noise of the data is reduced by averaging over an increasing number of realizations. The dotted line, above, shows the density profile if the walls are fixed.

cost of energy needed to deform the wall.

Mean-field theory

We demonstrate qualitatively the effect of wall fluctuations on the density profile by means of a simple mean-field calculation. We note that the symmetry of the geometry allows one to integrate out the x,y dependences and consider a z dependence along with an inversion symmetry. We map the repulsive part of the LJ potential into an effective hard sphere (EHS) system of diameter d [10] and treat the long-range attraction part perturbatively. Within the local density functional theory, the free energy will be given by [10]

$$F=\int_0^{H'/2}dz\rho(z)\ln\rho(z)-\frac{1}{2}\int_0^d dzdz'C_{HS}(z,z')\rho(z)\rho(z')$$
$$-\tfrac{1}{2}\int_d^{H'/2}dzdz'v_{LJ}^{att}(z,z')\rho(z)\rho(z')$$
$$+\int_0^{H'/2}V_{ext}(z)\rho(z).$$

Here $C_{HS}(z,z')$ is the Percus-Yevick direct correlation function [10] of the EHS and $v_{LJ}^{att}(z,z')$ is the long-range attractive part of the LJ interaction. We take $(H'/2)=(H/2)+\xi$, where ξ, assumed to be a Gaussian random variable with mean zero and standard deviation $\frac{1}{2}$, describes the fluctuations of the wall position. For a given realization of ξ, we solve numerically the self-consistency equation for $\rho(z)$, obtained by the stationarity condition of the free energy:

$$\rho(z)=\frac{1}{Z}\exp\left[\int_0^d dz'C_{HS}(z,z')\rho(z')\right.$$
$$\left.+\int_d^{H'/2}dz'v_{LJ}^{att}(z,z')\rho(z')-V_{ext}(z)\right],$$

where Z is determined by the normalization condition, namely, $2\int dz\rho(z)=1$. If we denote the self-consistent solution obtained for a given realization of ξ by $\rho_\xi(z)$, the average density profile is given by $\langle\rho(z)\rangle=\int d\xi P[\xi]\rho_\xi(z)$, where $P[\xi]$ is the normalized probability distribution of ξ. We show the theoretical density profiles in Fig. 5 for the bulk fluid phase with $H=10$, $K^*=0.01$. The dotted line in the figure shows the density profile that has peaks close to the walls if the walls have been fixed. $\langle\rho(z)\rangle$, obtained by averaging over 100 realizations of ξ, shows the washing out of the peaks close to the walls in qualitative agreement with the observations from the simulations, even though the details of the profile do not agree with the simulated ones. This could be related to the well-known limitations of the local density approximation in the context of confined geometry [11].

To summarize, our work is a theoretical attempt to show the important effects of the wall deformations on the static and dynamic properties of a fluid under confinement. Our predictions including that of the behavior of the MSD [Fig. 3(b)], which demonstrates the possibility of performing interesting dynamic light scattering experiments [12], can be verified in model systems reported in Ref. [4]. The dynamical behavior merits further understanding. We believe that our model would serve as a guide to a thorough theoretical understanding of the complicated behaviors exhibited by such systems. However, our model would require further improvements to this end: to extend it for the cases of low temperature and high density, and to include the nonlinear effects for large deformations.

ACKNOWLEDGMENTS

The author thanks H. Löwen for helpful discussions and OSPT for financial support. Shrabani Chakrabarti and B. V. R. Tata are gratefully acknowledged for critically reading the manuscript.

[1] M. Sliwinska-Bartkowiak, S. L. Sowers, and K. E. Gubbins, Langmuir **13**, 1182 (1997); J. Chakrabarti and P. J. A. M. Kerkhof (unpublished); K. G. Ayappa, Langmuir **14**, 880 (1998); S. A. Sommers *et al.*, J. Chem. Phys. **99**, 9890 (1993); M. Miyahara and K. E. Gubbins, *ibid.* **106**, 2865 (1997).

[2] R. Evans and U. M. B. Marconi, J. Chem. Soc., Faraday Trans. 1 **82**, 1763 (1986); B. K. Patterson, Jeremy P. R. B. Walton, and K. E. Gubbins, *ibid.* **82**, 1789 (1986), and references in these two papers.

[3] L. J. D. Frink and F. van Swol, J. Chem. Phys. **108**, 5588 (1998).

[4] K. P. Velikov, F. Durst, and O. D. Velev, Langmuir **14**, 1148 (1998), and references therein.

[5] The tangential components generally do not play a crucial role for overdamped systems as colloids [S. Ramaswamy (private communication)].

[6] The relevant quantity is the relative strength of deformation energy to a typical interparticle interaction parameter, which is ϵ here. With the stretching modulus of phospolipid membranes [V. Emsellem *et al.*, Phys. Rev. E **58**, 4807 (1998)] and LJ parameters for nearly spherical methane [S. Jiang *et al.*, J. Phys. Chem. **103**, 80 (1993)], for instance, $K^*\simeq 7.0$. This consideration is not specific to the interparticle interaction. For charge-stabilized colloidal dispersion confined by deformable walls, the rigidity energy would be compared to a typical interparticle interaction parameter, $Z^2e^2/\epsilon d$ [J. Chakrabarti and H. Lowen, Phys. Rev. E **58**, 3400 (1998)], with Z being the charge on the colloidal particles, e the fundamental charge, ϵ the dielectric constant of the dispersing solvent, and d the particle diameter. In this case the ratio could be varied over a wide range by tuning Z and d.

[7] The steep part of V_{ext}, assigned to a deformation equal to π [Fig. 1(b)], is introduced to ensure that no particle can leave the pore by the complete rupture of the walls. This guarantees the definition of the ensemble in our work.

[8] J. A. Barker and D. J. Henderson, J. Chem. Phys. **47**, 4714 (1967).

[9] B. V. R. Tata and A. K. Arora, J. Phys.: Condens. Matter **4**, 7699 (1992).

[10] J. P. Hansen and I. R. McDonald, *Theory of Simple Liquids* (Academic, New York, 1986).

[11] B. K. Peterson *et al.*, J. Chem. Phys. **88**, 6487 (1988).

[12] Bruce J. Berne and Robert Pecora, *Dynamic Light Scattering: With Applications to Chemistry, Biology, and Physics* (Wiley & Sons, New York, 1990).